



UNIVERSITY OF LEEDS

This is a repository copy of *Assessment of blending performance of pharmaceutical powder mixtures in a continuous mixer using Discrete Element Method (DEM)*.

White Rose Research Online URL for this paper:
<http://eprints.whiterose.ac.uk/157493/>

Version: Accepted Version

Article:

Alizadeh Behjani, M, Motlagh, YG, Bayly, AE orcid.org/0000-0001-6354-9015 et al. (1 more author) (2020) Assessment of blending performance of pharmaceutical powder mixtures in a continuous mixer using Discrete Element Method (DEM). *Powder Technology*, 366. pp. 73-81. ISSN 0032-5910

<https://doi.org/10.1016/j.powtec.2019.10.102>

© 2020 Elsevier B.V. All rights reserved. This manuscript version is made available under the CC-BY-NC-ND 4.0 license <http://creativecommons.org/licenses/by-nc-nd/4.0/>.

Reuse

This article is distributed under the terms of the Creative Commons Attribution-NonCommercial-NoDerivs (CC BY-NC-ND) licence. This licence only allows you to download this work and share it with others as long as you credit the authors, but you can't change the article in any way or use it commercially. More information and the full terms of the licence here: <https://creativecommons.org/licenses/>

Takedown

If you consider content in White Rose Research Online to be in breach of UK law, please notify us by emailing eprints@whiterose.ac.uk including the URL of the record and the reason for the withdrawal request.



eprints@whiterose.ac.uk
<https://eprints.whiterose.ac.uk/>

Journal Pre-proof

Assessment of blending performance of pharmaceutical powder mixtures in a continuous mixer using Discrete Element Method (DEM)

Mohammadreza Alizadeh Behjani, Yousef Ghaffari Motlagh, Andrew Bayly, Ali Hassanpour



PII: S0032-5910(19)30931-3

DOI: <https://doi.org/10.1016/j.powtec.2019.10.102>

Reference: PTEC 14869

To appear in: *Powder Technology*

Received date: 4 June 2019

Revised date: 25 October 2019

Accepted date: 26 October 2019

Please cite this article as: M.A. Behjani, Y.G. Motlagh, A. Bayly, et al., Assessment of blending performance of pharmaceutical powder mixtures in a continuous mixer using Discrete Element Method (DEM), *Powder Technology*(2019), <https://doi.org/10.1016/j.powtec.2019.10.102>

This is a PDF file of an article that has undergone enhancements after acceptance, such as the addition of a cover page and metadata, and formatting for readability, but it is not yet the definitive version of record. This version will undergo additional copyediting, typesetting and review before it is published in its final form, but we are providing this version to give early visibility of the article. Please note that, during the production process, errors may be discovered which could affect the content, and all legal disclaimers that apply to the journal pertain.

© 2019 Published by Elsevier.

Assessment of blending performance of pharmaceutical powder mixtures in a continuous mixer using Discrete Element Method (DEM)

Mohammadreza Alizadeh Behjani, Yousef Ghaffari Motlagh, Andrew Bayly, Ali Hassanpour*

School of Chemical and Process Engineering, University of Leeds, Leeds, UK.

*Corresponding author:

Tel: +44(0)113 343 2405

A.Hassanpour@leeds.ac.uk

Abstract

This study proposes a new sample-independent mixing index, termed the Coefficient of Blending Performance (CBP), for monitoring the formation of undesired API (Active Pharmaceutical Ingredient) agglomerates in continuous mixing processes. The sensitivity of the proposed index is tested on a DEM-simulated twin-screw blending of pharmaceutical powders with a novel mixing design. Model excipient and API are used in simulations with their physical and mechanical properties being within the typical range of properties of generic pharmaceutical powders. Results suggest that the CBP is an effective index for monitoring the formation of API agglomerates in the mixer. Using this index, DEM results suggest a high possibility of formation of API agglomerates during the first stage of twin screw mixing. The results show that adding a kneading zone to the twin screw mixer enhances the blending quality by breaking the API agglomerates, making the mixture ready for the next operating unit.

Key words: Twin screw mixer, Discrete Element Method, Active Pharmaceutical Ingredient, mixing index; agglomeration; surface energy

1 Introduction

Securing a high-quality granular blending/mixing is a vital step for many industries, and designing suitable and efficient mixers is central for delivering a homogeneous mixture. Mixer design depends on the nature of an industry, type of material, desired production rate, and the maximum acceptable variance in the product composition. This includes the mixer geometrical aspects, such as the blades/impellers shape and the mixer size as well as the operating mechanisms, namely the type of mixing (batch or continuous) and the power input per unit mass [1-7]. There are various types and models of mixers available which can be classified into two main categories of batch and continuous, each of which has its own advantages and disadvantages [8]. Although in recent decades the process of designing mixers has become more scientific, they still fall short in meeting the needs of industries, and compared to the effort put into mixing the outcome is not as satisfying [9, 10]. The pharmaceutical industry is one of those industries which benefit the most from enhancement in the quality of mixers.

In pharmaceutical processing, Active Pharmaceutical Ingredient (API) is usually mixed with excipient for the formulation of the final products. API particles are very fine ($< 5\mu\text{m}$) and as a result, their attractive electrostatic and van der Waals forces are very large compared to their inertial forces (high granular Bond number [11]), contributing to their high cohesivity and poor flowability [12, 13]. The API particles are commonly mixed with a large quantity of excipient materials to increase their flowability and dispersion efficiency; nevertheless, during the blending process, the cohesive fine particles stick to each other and form agglomerates. These agglomerates are not generally desirable, because they change the homogeneity and size distribution of the mixture. To enhance the efficiency of blending, understanding the underlying mechanisms and the tendency of formation of API-API agglomerates at each stage of the blending process is highly crucial.

The conventional experimental methods for assessing the efficiency of blending in a mixer are mainly based on the variance of particles concentration in the mixture [14-16]. To find a

component concentration, sampling is needed. Evidently, changing the sample size and sampling methodology affects the value of concentration variance. Size of a sample is commonly defined based on the scale of scrutiny, which depends on the application of the powder mixture. In spite of the prevalent usage of sample-dependent methods, some features of mixing/segregation process, e.g. the agglomeration of API particles, cannot be captured by these methods. It is utterly difficult and expensive to experimentally assess the spatial homogeneity of a mixture in a non-destructive way; however, using modelling techniques based on Discrete Element Method (DEM) it is possible to monitor particle contacts and formation/breakage of agglomerates, from which the aforementioned assessments can be easily conducted. Chandratilleke et al. [17] proposed a sample-independent index for assessing quality of DEM simulated powder mixtures. Although their method works well for monosized particulate systems, it is not applicable for evaluating binary systems or mixtures in which particles have size distribution. Even though tracking particle collisions and contacts is feasible in DEM, there is still a lack of a suitable criterion/index for monitoring the formation of agglomerates during mixing.

The emergence and development of the DEM technique has paved the road towards designing more efficient and practical mixers. So far, the blending process in different types of mixers/blenders, namely the simple-rotating drums [18, 19], tumbling blenders [20-22], bin blender [23], v-blenders [24-27], twin screw mixer [28], tote blenders [29, 30], paddle mixers [31], double-cone blender [32], slant cone mixers [33, 34], agitated tubular mixer [35], bladed mixers [5, 7, 17, 36, 37], and ribbon mixer [38], has been simulated using DEM. Continuous mixing is receiving more and more attention by pharmaceutical industries due to its advantages over the batch mixing. Among the continuous mixers, twin screw mixers have shown great potential in pharmaceutical manufacturing processes owing to their flexibility in design, low throughput, and relatively short residence time. Powder mixing with twin screw is a variant of high-shear mixing where extruders are installed to blend the powders in a continuous manner [39]. In spite of their ever-rising popularity, investigations on the agglomeration of low-level content APIs during the continuous mixing are still lacking. In this regard, defining a versatile criterion to quantify the rate of formation of these undesired agglomerates is necessary.

Apart from the design and quality of a mixer, the particles physical and mechanical properties also play a significant role in the quality of the final mixture. The particles size [7], size distribution [40, 41], shape [42, 43], density [7], and surface energy [44] are all amongst the most influential properties to be mentioned [7]. The significance of each property is also a function of other properties; for example, when particles are very fine the adhesive forces related to the surface energy become dominate, which eventually lead to their agglomeration and/or segregation in the mixture.

In this study the process of blending of pharmaceutical powders in a continuous twin screw mixer is studied using DEM technique. To monitor and analyse the formation/breakage of the API agglomerates, a sample-independent mixing index is proposed based on the number of contacts of similar and dissimilar particles. The sensitivity of the blending process to the operating conditions, such as mixer design and impeller rotational speed, as well as material properties, i.e. particles surface adhesion, is investigated. The proposed index is compared to the commonly used relative standard deviation (RSD) method for selected cases of the simulations.

2 Computational methodology

DEM is a method for modelling the dynamic behaviour of assemblies of individual elements. This method, initially developed and used for geotechnical problems by Cundall and Strack [45], is now used extensively in various fields of engineering, particularly for simulation of powder handling and processing. In DEM, particle movements are predicted by using the Newton's second law of motion in translational and rotational forms and the particles interactions are defined using appropriate contact models [46]. In this study, EDEM 2.7.1 software, provided by DEM Solutions, Edinburgh, UK, is utilised to simulate the blending process.

2.1 Contact models

Particles collisional forces are generally divided into normal and tangential components, where the normal term is calculated based on the Hertz model [47] and the tangential term is obtained using the Mindlin theory [48]. More details for these theories are available elsewhere [46, 49]. As mentioned before, the pharmaceutical particles are generally cohesive and very fine;

therefore, their inter-particle attractive forces have to be taken into account. To consider the effect of adhesion on particles interactions, the JKR (Johnson-Kendall-Roberts) [50] model is used. This model is an elastic non-linear model and is generally suitable for soft materials, in comparison with the DMT model [51], which is mostly utilised for hard materials.

One of the main issues with using adhesive contact models is how to translate the level of adhesivity of particles to a meaningful parameter in DEM simulations, e.g. which value should be selected for the particles interfacial energy. In addition to the surface energy, the adhesive forces present between two particles depend on their material properties, size, shape, and surface roughness as well. In DEM simulations, using particles with larger size, simplified shapes, and lower Young's modulus is inevitable, owing to the high computational demand of the DEM. Thus, the interfacial energy used in simulations should be a scaled version of its real value by which similar bulk behaviour to that of the experimental one is achievable. For this purpose, Behjani et al. [52] recently proposed a dimensionless Cohesion number for inferring the particles interfacial energy with respect to their scaled size and stiffness. This number is defined based upon the work of cohesion required for detaching a particle from a surface over its gravitational potential energy, as expressed in Equation (1),

$$C_{coh} = \frac{1}{\rho g} \left(\frac{\Gamma^5}{E^* R^{*8}} \right)^{1/3} \quad (1)$$

where g , ρ , and Γ are gravitational acceleration, envelope density, and interfacial energy of the particles respectively. R^* and E^* are the reduced radius and Young's modulus of elasticity of the spheres, respectively:

$$R^* = \left(\frac{1}{R_1} + \frac{1}{R_2} \right)^{-1} \quad (2)$$

$$E^* = \left(\frac{1 - \nu_1^2}{E_1} + \frac{1 - \nu_2^2}{E_2} \right)^{-1} \quad (3)$$

where R_1 and R_2 are the radii of the spheres, E_1 and E_2 are their Young's moduli, and ν_1 and ν_2 are their Poisson's ratios. This method of scaling has been used in other researches successfully [53-55].

Two model materials, i.e. an API and excipient, are considered in the formulation of the target pharmaceutical powder mixture. The material properties of these model particles are extracted from the literature in a way to resemble two common pharmaceutical ingredients, i.e.

Paracetamol as the API and Lactose as the excipient. The average values found in the literature are used in calibration of the DEM input parameters, as given in Table 1.

The geometry used in the simulations belongs to a twin screw mixer displayed in Fig. 1. It consists of an initial long mixing zone and a kneading zone, followed by a short secondary mixing zone. This geometry is built using the open source meshing generator software, *Gmsh*, and the *.stl* mesh file is exported to the EDEM software. In the EDEM software, the particles are generated and discharged into the funnel located on the left hand side of the mixer and then introduced into the mixer according to the feed rate mentioned in Table 2. Afterwards, the rotating screws mix the particles and push them gradually to the exit.

2.3 Simulation setup

The particles input parameters used in the simulations are given in Table 2. To reduce the computation time, lower Young's modulus values and larger particle diameters are used compared to their real experimental values. To find a suitable value for the interfacial energy of the scaled particles the Cohesion number is used as described in section 2.1. For scaling the surface energy, the value of the Cohesion number using the real particle properties (Table 1) should be equated with that of the simulation as expressed below:

$$Coh_{exp} = Coh_{sim} = \frac{1}{\rho_{sim}g} \left(\frac{\Gamma_{sim}^5}{E_{sim}^2 R_{sim}^8} \right)^{1/3} = \frac{1}{\rho_{exp}g} \left(\frac{\Gamma_{exp}^5}{E_{exp}^2 R_{exp}^8} \right)^{1/3} \quad (4)$$

where indices *exp* and *sim* denote experimental and simulation, respectively. The Cohesion number is around 2.9 for realistic particles properties as given in Table 3. Using a similar value for the Cohesion number of the scaled particles, i.e. simulated particles, with their new Young's modulus and particle size, the interfacial energy of the API (e.g. Paracetamol-Paracetamol) is approximately 400 mJm^{-2} in DEM modelling.

In total, three values are used for the interfacial energy to study the effect of particle adhesivity on mixing quality. It should be mentioned that the excipient interfacial energy is maintained low (40 mJm^{-2}) and constant for all cases in this study in order to only study the effect of API properties. Also, the API-excipient interfacial energy is taken as the average of the API and excipient surface energies.

The speed at which the process of mixing is conducted can cause a significant difference in the final quality of the mixture. For this to be studied, simulations are carried out using 500, 600, and 700 rpm rotational speeds of the mixer as presented in Table 2. The feed rates of the API and excipient are kept constant at 7.2 and 0.72 gs^{-1} , respectively, for all the rotational speeds (9% API and 91% excipient by mass). The feed consists of approximately 9% API and 91% excipient, which is in a range of the feed ratio that is normally used by pharmaceutical industries. Variation in feed ratio may have an impact on blending performance, however, it is not studied in this work.

3 Mixing quantification

There are various ways in the literature to quantify the quality of a mixture most of which are based on the variance of the components mass/volume concentration [14-16]. The relative standard deviation (RSD), which is the ratio of the standard deviation of a variable over its mean value, is a common index utilised by researchers and engineers [42]. In spite of being widely used, this index is highly dependent on the sampling method and sample size, both of which are sources of uncertainty.

In this study, the whole mixer is divided into number of bins as presented in Fig. 2. As shown in the figure, the cross section of the mixer geometry is divided into bins based on the radial symmetry of the mixer, so that all the bins have equal chance for accommodation particles. This is performed to avoid variation in sample size, which is a source for uncertainty in the final results. The mass concentrations of the API and excipient particles, C_i , are calculated in each bin using Equation (5).

$$C_i = \frac{m_i}{\sum m_i} \quad (5)$$

where m_i is the mass of component i in the bin. Using the concentration values obtained for all the bins, the RSD of the API and excipient are determined using Equation (6),

$$RSD = \frac{SD}{\bar{C}} = \frac{\sqrt{\frac{\sum_1^N (C_i - \bar{C})^2}{N - 1}}}{\frac{1}{N} \sum_1^N C_i} \quad (6)$$

where SD stands for the standard deviation of the concentrations, \bar{C} is their mean value, and N is the number of bins.

Due to the complexity of the geometry of the mixer, only two bin sizes are defined for calculating the RSD values. Discretising the mixture to smaller samples will lead to the formation of semi-empty bins and a non-homogeneous sampling. In other words, some bins cannot be completely filled by particles because of the intervening and dynamic geometry or due to the location of the bin. Here, as presented in Fig. 2, the cross section of the mixer is divided into equal sections based on the radial symmetry of the mixer to reduce the sampling issue. This issue can also be addressed by analysing the variation of composition of the discharging mixture at the outlet of the mixer throughout the blending time. Nevertheless, this method is still sample-dependent, i.e. the RSD alters with changing the scale of scrutiny. It is a fact that relying on sample-dependent indices for analysing a mixture quality can sometimes be misleading. As illustrated in Fig. 3, the composition ratios of the API and excipient in the bins are similar for the three cases presented, based on which the RSD for all these cases would be similarly low ($0.09 \leq RSD \leq 0.11$). In the first two cases, shown in Fig. 3 (A) and (B), changing the size or arrangement of the bins may vary the RSD value significantly. For example, in the cases A and B if each bin is divided with a horizontal line into two similar bins (i.e. reducing bin size to half of its original size) the RSD jumps from 0.11 up to 0.33., while, this value increases only to 0.14 for the case C. To solve the sampling issue and also be able to analyse the formation and depletion of API agglomerates during the blending, two new indices are defined based on the number of contacts of similar and dissimilar particles, i.e. API-API and API-excipient. These indices are shown in Equations (7) and (8).

$$CR_{Ae} = \frac{N_{Ae}}{N_e} \quad (7)$$

$$CR_{AA} = \frac{N_{AA}}{N_A} \quad (8)$$

CR_{Ae} shows the ratio of the API-excipient contact number over the total number of excipient particles, and CR_{AA} is the ratio of API-API contacts over the total number of API particles. These values are calculated for the cases with different operating conditions and the results are compared. As a final evaluating step, the ratio of the CR_{Ae} and CR_{AA} is defined as the coefficient of blending performance (CBP), as expressed in Equation (9), by which the efficient blending scenarios are more easily distinguished.

$$CBP = \frac{CR_{Ae}}{CR_{AA}} = \frac{N_{Ae} N_e}{N_{AA} N_A} \quad (9)$$

It is noteworthy that CBP can be used for assessing mixtures which have monosized particles as well as particles of different sizes and even with a size distribution.

4 Results and discussion

4.1 Effect of twin screw mixer geometry

The geometry of a mixer is undoubtedly one of the most important factors in its performance. Conventional twin screw mixers contain a section to mix particles with each other and deliver a well-mixed system at the end of the process. However, there is a high chance of agglomeration of fine particles while interacting with each other. To overcome this issue, a new geometry for twin screw mixing is proposed, which consists of a kneading zone and a secondary mixing zone as well. The effect of incorporating the kneading zone and secondary mixing zone into the base model on the efficiency of mixing and formation and breakage of agglomerates is studied.

4.1.1 Steady state condition

Mass hold-up in the TSM is monitored versus time to evaluate the steady state conditions. As presented in Fig. 4, the mass hold-up in the TSM increases constantly till $t=27$ s, after which hold-up gradually plateaus, which shows that the process has reached a steady state. The

Overall hold-up (mass) values in both cases are very similar, suggesting similar volumetric fill levels of the mixer in both cases. It should be noted that the excipient's hold-up reaches the steady state slightly earlier than that of the API. Furthermore, increasing the interface energy of the API particles has caused a slight reduction in accumulation of APIs in the TSM, suggesting that higher stickiness of constituents helps in maintaining the composition ratio of the mixture.

4.1.2 Blending assessment using RSD

To evaluate the effect of various sections of the twin screw mixer on blending quality, the RSD of mass concentrations of the API and excipient particles is calculated. Two bin sizes are used, as shown in Fig. 2, to consider the effect of sample size on the RSD. Large bins contain around 800 particles each, and small bins have less than 80 particles on average. As presented in Fig. 5, the RSD values for the API particles are much higher than those of the excipients. It is observed that using fine bins in the sampling has increased the API and excipient RSD values by two times. This is because reducing the size of the scale of scrutiny lowers the number of particles in each sample which is directly associated with the randomness of the particles composition ratio. In other words, higher variability in particles composition ratio is expected when the sample size is reduced. Nevertheless, the RSD values are found to be insensitive to the mixer geometry, i.e. no change in the RSD values is observed when particles move from one section to another, either for the coarse or the fine bins.

4.1.3 Blending assessment using the contact ratios (CR)

To evaluate the particles' arrangements more closely, contact ratios of the particles are calculated as well and presented in Fig. 6 and Fig. 7. Lower values for the CR_{AA} and higher ones for the CR_{Ae} are indications of a more uniformly mixed system. As it is clear in Fig. 6, for all the cases simulated, kneading zone has the lowest CR_{AA} compared to the first and the second mixing zones. Also, it is observed that the number of API-API contacts has increased largely in the second mixing zone. This means that adding the secondary mixing zone to the whole mixer has practically deteriorated the blending quality and hence is useless.

A confirmation for the positive effect of the kneading zone can be observed in the results of the CR_{Ae} in Fig. 7. This graph shows that for most of the simulations the maximum contact number of the API and excipient particles occurs in the kneading zone. The higher API-API contact ratio in the mixing zones are due to their high cohesivity which leads to their local accumulation and agglomeration; this can be easily observed through the particles distribution in the mixer as presented in Fig. 8. Local accumulation of the API particles in the first and second mixing zones is evident, particularly close to the areas which experience high shear rates like the screw walls. On the other hand, the kneading zone shows a more uniform particle distribution corroborating the quantitative results.

4.2 Effect of the particle surface energy

The effect of the surface condition of particles on the final quality of the mixture is studied by doing simulations with three various values of the surface energy. Looking at Fig. 6 and Fig. 7, a general increasing trend for the contact ratios is observed at the mixing zones 1 and 2 when the surface energy is increased. This is not the case for the kneading zone, where the trends differ from one rotational speed to another. For the CR_{Ae} , there is an increasing trend at the 500 rpm while for the 600 and 700 rpm the lowest CR_{Ae} occurs when the surface energy is 400 mJ/m^2 .

It is also worth to mention that the role of the kneading zone in improving the quality of the mixture is more observable when the surface energy is lower; i.e. the highest increase in the values of the CR_{Ae} are obtained at the lowest surface energy values.

4.3 Effect of the mixer rotation rate

The mixer rotation rate is an important operating parameter which affects the quality of mixing as well as the speed of the process. For the surface energy values of 200, 400, and 800 mJ/m^2 the API-API and API-excipient contact ratios are calculated at various rotational speeds of the mixer. As depicted in Fig. 9, a unique trend for the CR_{AA} and CR_{Ae} cannot be observed. For the first mixing zone, a general increasing trend for the API-API contacts is observed when the

rotational speed is increased. The CR_{Ae} of the same mixing zone shows a decreasing trend with a minimum value at 600 rpm followed by a slight increase at 700 rpm. At the Kneading zone, however, both CR_{AA} and CR_{Ae} show similar decreasing-increasing trends with slight variations. Here the optimum rotational rate cannot be easily found, nevertheless, based on the CR_{AA} , 600 rpm rotational speed shows a better performance in terms of breaking the API-API agglomerates.

4.3.1 Blending assessment using CBP index

Variance-based indices, like the RSD, are useful tools for assessing the spatial distribution of mixture components. The extent of variability in the composition ratio of species is the base for these indices and highly influenced by sampling methodology. Regardless of the aforementioned drawback, such indices are fundamentally incapable of giving information about particles arrangement in a sample. In this regard, an undesired phenomenon during the blending process of pharmaceutical powders is the agglomeration of APIs, which is hard to monitor experimentally. Monitoring this phenomenon, however, is feasible by DEM analysis, albeit by using a suitable index. The coefficient of blending performance, CBP, is an index which provides information on the contact number of similar and dissimilar species. Variation in this index is an indication of formation or breakage of undesired agglomerates.

To have a better understanding of the performance of blending in each section of the twin screw mixer, CBP is calculated at various particle surface energies and mixer rotational speeds, as presented in Fig. 10. Clearly, the highest CBP values for the CBP are achieved by far at the kneading zone, where the $CBP \geq 4$ at 200 and 400 mJ/m^2 surface energies. These values drop slightly when the surface energy is increased to 800 mJ/m^2 . On the other hand, the lowest CBP values observed belong to the second mixing zone, where the blending performance remains nearly constant at $CBP=1$ for all the surface energy values and rotational speeds. The first mixing zone, however, has a different behaviour, where the best performance of the mixing zone 1 is achieved at 500 rpm rotational speed, and as the rotational speed increases the CBP decreases. Also, the CBP values reduce slightly when the surface energy of the particles is

increased. A clear advantage of using CBP in this study was its sample-independent nature, making it a robust and reliable approach for assessing the mixture quality.

5 Conclusions

High-quality mixing of pharmaceutical powders has two aspects: 1) uniform distribution of all ingredients and 2) minimal formation of undesired API agglomerates. There is still a lack of a rigorous methodology for the assessment of the agglomeration of low-level content API within continuous mixers. Along with the traditional variance-based RSD index, a sample-independent index, CBP, is proposed for assessing the formation of undesired API agglomerates. To examine the efficacy of this index, a case study is conducted about the effect of geometry design on blending performance of a continuous twin screw mixer, using DEM simulations. Also, the sensitivity of the blending process to the mixer rotation rate and particles cohesivity/adhesivity is examined using the proposed index.

The results suggest that the coefficient of blending performance (CBP) has the capability to capture the formation of agglomerates within the mixer; while this cannot be observed using the RSD index. Based on the CBP results, the best blending performance is achieved in the kneading zone; whereas, the poorest mixture quality (the highest number of agglomerates) is observed in the second mixing zone. This indicates that by adding the kneading zone to the design of a conventional TSM, the API agglomerates which are formed during the blending process break down to their original form before being fed into the next operating unit. In contrast, adding the second mixing zone to the operation reduces the mixture quality significantly. At the first mixing zone, the best blending performance is obtained when the rotational speed is the lowest (500 rpm), however, the dependence of the blending performance on mixer rotational speed is not considerable at the kneading and second mixing zones. In addition, variation in the CBP does not follow a unique trend when differing the adhesivity of the components in various sections of the mixer.

Acknowledgment

We gratefully acknowledge the support of the Advanced Manufacturing Supply Chain Initiative through the funding of the ADDoPT project (Advanced Digital Design of Pharmaceutical Therapeutics) [Grant No. 14060] which has enabled us to develop robust tools for prediction and analysis of continuous blending of pharmaceutical powders”

6 References

- [1] K. Terashita, T. Nishimura, S. Natsuyama, Optimization of operating conditions in a high-shear mixer using DEM model: Determination of optimal fill level, *Chem Pharm Bull*, 50 (2002) 1550-1557.
- [2] A. Santomaso, M. Olivi, P. Canu, Mechanisms of mixing of granular materials in drum mixers under rolling regime, *Chem Eng Sci*, 59 (2004) 3269-3280.
- [3] G.R. Chandratilleke, A.B. Yu, R.L. Stewart, J. Bridgwater, Effects of blade rake angle and gap on particle mixing in a cylindrical mixer, *Powder Technol*, 193 (2009) 303-311.
- [4] S.S. Manickam, R. Shah, J. Tomei, T.L. Bergman, B. Chaudhuri, Investigating mixing in a multi-dimensional rotary mixer: Experiments and simulations, *Powder Technol*, 201 (2010) 83-92.
- [5] B. Remy, B.J. Glasser, J.G. Khinast, The Effect of Mixer Properties and Fill Level on Granular Flow in a Bladed Mixer, *AIChE J*, 56 (2010) 336-353.
- [6] M.Q. Jiang, Y.Z. Zhao, G.S. Liu, J.Y. Zhang, Enhancing mixing of particles by baffles in a rotating drum mixer, *Particuology*, 9 (2011) 270-278.
- [7] H. Musha, G.R. Chandratilleke, S.L.I. Chan, J. Bridgwater, A.B. Yu, Effects of Size and Density Differences on Mixing of Binary Mixtures of Particles, *Aip Conf Proc*, 1542 (2013) 739-742.
- [8] S. Oka, A. Sahay, W. Meng, F. Muzzio, Diminished segregation in continuous powder mixing, *Powder Technol*, 309 (2017) 79-88.
- [9] J. Bridgwater, Mixing of particles and powders: Where next?, *Particuology*, 8 (2010) 563-567.
- [10] J. Bridgwater, Mixing of powders and granular materials by mechanical means-A perspective, *Particuology*, 10 (2012) 397-427.
- [11] M. Capece, R. Ho, J. Strong, P. Gao, Prediction of powder flow performance using a multi-component granular Bond number, *Powder Technol*, 286 (2015) 561-571.
- [12] J. Yang, C.-Y. Wu, M. Adams, DEM analysis of particle adhesion during powder mixing for dry powder inhaler formulation development, *Granular Matter*, 15 (2013) 417-426.
- [13] M. Alizadeh Behjani, M. Pasha, H. Lu, C. Hare, A. Hassanpour, Chapter 3 Prevailing Conditions of Flow in Particulate Systems, *Powder Flow: Theory, Characterisation and Application*, The Royal Society of Chemistry 2019, pp. 39-63.

- [14] S.-H. Chou, T.-L. Song, S.-S. Hsiao, A study of the mixing index in solid particles, *KONA Powder and Particle Journal*, (2016) 2017018.
- [15] P.M.C. Lacey, The mixing of solid particles, *Chemical Engineering Research and Design*, 75 (1997) S49-S55.
- [16] L.T. Fan, R.H. Wang, On mixing indices, *Powder Technol*, 11 (1975) 27-32.
- [17] G.R. Chandratilleke, A.B. Yu, J. Bridgwater, K. Shinohara, A particle-scale index in the quantification of mixing of particles, *Aiche J*, 58 (2012) 1099-1118.
- [18] G. Baumann, I.M. Jánosi, D.E. Wolf, Particle Trajectories and Segregation in a Two-Dimensional Rotating Drum, *EPL (Europhysics Letters)*, 27 (1994) 203.
- [19] H. Ahmadian, A. Hassanpour, M. Ghadiri, Analysis of granule breakage in a rotary mixing drum: Experimental study and distinct element analysis, *Powder Technol*, 210 (2011) 175-180.
- [20] M. Moakher, T. Shinbrot, F.J. Muzzio, Experimentally validated computations of flow, mixing and segregation of non-cohesive grains in 3D tumbling blenders, *Powder Technol*, 109 (2000) 58-71.
- [21] B. Chaudhuri, A. Mehrotra, F.J. Muzzio, M.S. Tomassone, Cohesive effects in powder mixing in a tumbling blender, *Powder Technol*, 165 (2006) 105-114.
- [22] T. Shinbrot, M. Zeggio, F.J. Muzzio, Computational approaches to granular segregation in tumbling blenders, *Powder Technol*, 116 (2001) 224-231.
- [23] M. Lemieux, F. Bertrand, J. Chaouki, P. Gosselin, Comparative study of the mixing of free-flowing particles in a V-blender and a bin-blender, *Chem Eng Sci*, 62 (2007) 1783-1802.
- [24] A. Alexander, F.J. Muzzio, T. Shinbrot, Segregation patterns in V-blenders, *Chem Eng Sci*, 58 (2003) 487-496.
- [25] J. Doucet, F. Bertrand, J. Chaouki, Experimental characterization of the chaotic dynamics of cohesionless particles: application to a V-blender, *Granular Matter*, 10 (2008) 133-138.
- [26] M. Lemieux, G. Léonard, J. Doucet, L.A. Leclaire, F. Viens, J. Chaouki, F. Bertrand, Large-scale numerical investigation of solids mixing in a V-blender using the discrete element method, *Powder Technol*, 181 (2008) 205-216.
- [27] D. Brone, A. Alexander, F.J. Muzzio, Quantitative characterization of mixing of dry powders in V-blenders, *Aiche J*, 44 (1998) 271-278.
- [28] F. Qi, T.J. Heindel, M.M. Wright, Numerical study of particle mixing in a lab-scale screw mixer using the discrete element method, *Powder Technol*, 308 (2017) 334-345.
- [29] P.E. Arratia, N.-h. Duong, F.J. Muzzio, P. Godbole, S. Reynolds, A study of the mixing and segregation mechanisms in the Bohle Tote blender via DEM simulations, *Powder Technol*, 164 (2006) 50-57.
- [30] O.S. Sudah, P.E. Arratia, A. Alexander, F.J. Muzzio, Simulation and experiments of mixing and segregation in a tote blender, *Aiche J*, 51 (2005) 836-844.

- [31] A. Hassanpour, H.S. Pan, A. Bayly, F. Gopalakrishnan, D. Ng, M. Ghadiri, Analysis of particle motion in a paddle mixer using Discrete Element Method (DEM), *Powder Technol*, 206 (2011) 189-194.
- [32] A.W. Alexander, T. Shinbrot, F.J. Muzzio, Granular segregation in the double-cone blender: Transitions and mechanisms, *Physics of Fluids (1994-present)*, 13 (2001) 578-587.
- [33] B. Alchikh-Sulaiman, F. Ein-Mozaffari, A. Lohi, Evaluation of poly-disperse solid particles mixing in a slant cone mixer using discrete element method, *Chem Eng Res Des*, 96 (2015) 196-213.
- [34] M. Alian, F. Ein-Mozaffari, S.R. Upreti, J.N. Wu, Using discrete element method to analyze the mixing of the solid particles in a slant cone mixer, *Chem Eng Res Des*, 93 (2015) 318-329.
- [35] Y. He, A.E. Bayly, A. Hassanpour, F. Muller, K. Wu, D. Yang, A GPU-based coupled SPH-DEM method for particle-fluid flow with free surfaces, *Powder Technol*, 338 (2018) 548-562.
- [36] S. Radl, E. Kalvoda, B.J. Glasser, J.G. Khinast, Mixing characteristics of wet granular matter in a bladed mixer, *Powder Technol*, 200 (2010) 171-189.
- [37] B. Remy, J.G. Khinast, B.J. Glasser, Discrete Element Simulation of Free Flowing Grains in a Four-Bladed Mixer, *Aiche J*, 55 (2009) 2035-2048.
- [38] G. Basinskas, M. Sakai, Numerical study of the mixing efficiency of a ribbon mixer using the discrete element method, *Powder Technol*, 287 (2016) 380-394.
- [39] A. Chaudhury, D. Barrasso, D.A. Pohlman, J.D. Litster, R. Ramachandran, 5 - Mechanistic modeling of high-shear and twin screw mixer granulation processes, in: P. Pandey, R. Bharadwaj (Eds.) *Predictive Modeling of Pharmaceutical Unit Operations*, Woodhead Publishing 2017, pp. 99-135.
- [40] J.F. Li, C. Wassgren, J.D. Litster, Multi-scale modeling of a spray coating process in a paddle mixer/coater: the effect of particle size distribution on particle segregation and coating uniformity, *Chem. Eng. Sci*, 95 (2013) 203-210.
- [41] A. Shimosaka, Y. Shirakawa, J. Hidaka, Effects of Particle Shape and Size Distribution on Size Segregation of Particles, *J Chem Eng Jpn*, 46 (2013) 187-195.
- [42] M. Alizadeh, A. Hassanpour, M. Pasha, M. Ghadiri, A. Bayly, The effect of particle shape on predicted segregation in binary powder mixtures, *Powder Technol*, 319 (2017) 313-322.
- [43] M.D. Sinnott, P.W. Cleary, The effect of particle shape on mixing in a high shear mixer, *Computational Particle Mechanics*, 3 (2016) 477-504.
- [44] R. Brewster, G.S. Grest, A.J. Levine, Effects of cohesion on the surface angle and velocity profiles of granular material in a rotating drum, *Physical Review E*, 79 (2009) 011305.
- [45] P.A. Cundall, O.D. Strack, A discrete numerical model for granular assemblies, *Geotechnique*, 29 (1979) 47-65.
- [46] M.M. Martín, *Introduction to software for chemical engineers*, CRC Press 2014.
- [47] H. Hertz, Ueber die Berührung fester elastischer Körper (on the contact of elastic solids), *Journal für die reine und angewandte Mathematik (Crelle's Journal)*, 1882, pp. 156–171.

- [48] H. Deresiewicz, H.D. Mindlin, C. Columbia, E. Department of Civil, Elastic Spheres in contact under varying oblique forces, 1952.
- [49] A. Di Renzo, F.P. Di Maio, Comparison of contact-force models for the simulation of collisions in DEM-based granular flow codes, *Chem Eng Sci*, 59 (2004) 525-541.
- [50] K.L. Johnson, K. Kendall, A.D. Roberts, Surface Energy and the Contact of Elastic Solids, *Proceedings of the Royal Society of London A: Mathematical, Physical and Engineering Sciences*, 324 (1971) 301-313.
- [51] B.V. Derjaguin, V.M. Muller, Y.P. Toporov, Effect of contact deformations on the adhesion of particles, *Journal of Colloid and Interface Science*, 53 (1975) 314-326.
- [52] M.A. Behjani, N. Rahmanian, N. Fardina bt Abdul Ghani, A. Hassanpour, An investigation on process of seeded granulation in a continuous drum granulator using DEM, *Advanced Powder Technology*, 28 (2017) 2456-2464.
- [53] M. Alizadeh Behjani, A. Hassanpour, M. Ghadiri, A. Bayly, Numerical Analysis of the Effect of Particle Shape and Adhesion on the Segregation of Powder Mixtures, *EPJ Web Conf.*, 140 (2017) 06024.
- [54] W. Nan, M. Pasha, T. Bonakdar, A. Lopez, U. Zafar, S. Nadimi, M. Ghadiri, Jamming during particle spreading in additive manufacturing, *Powder Technol*, 338 (2018) 253-262.
- [55] M. Alizadeh, M. Asachi, M. Ghadiri, A. Bayly, A. Hassanpour, A methodology for calibration of DEM input parameters in simulation of segregation of powder mixtures, a special focus on adhesion, *Powder Technol*, 339 (2018) 789-800.
- [56] A.-S. Persson, H. Ahmed, S. Velaga, G. Alderborn, Powder Compression Properties of Paracetamol, Paracetamol Hydrochloride, and Paracetamol Cocrystals and Coformers, *Journal of Pharmaceutical Sciences*, 107 (2018) 1920-1927.
- [57] U.V. Shah, Z. Wang, D. Olusami, A.S. Narang, M.A. Hussain, M.J. Tobyn, J.Y.Y. Heng, Effect of milling temperatures on surface area, surface energy and cohesion of pharmaceutical powders, *International Journal of Pharmaceutics*, 495 (2015) 234-240.
- [58] S. Pazesh, A.-S. Persson, J. Berggren, G. Alderborn, Effect of milling on the plastic and the elastic stiffness of lactose particles, *European Journal of Pharmaceutical Sciences*, 114 (2018) 138-145.
- [59] T. Beyer, G.M. Day, S.L. Price, The Prediction, Morphology, and Mechanical Properties of the Polymorphs of Paracetamol, *Journal of the American Chemical Society*, 123 (2001) 5086-5094.

Table captions

Table 1. Physical and mechanical properties of the common pharmaceutical ingredients [56-59].

Table 2. Physical properties of the API and excipient particles used in the DEM simulations.

Table 3. The table used to scale the surface energy of the API particles in the DEM simulations.

Figure captions

- Fig. 1. The top, side, and front views of the mixer geometry used in the simulations.
- Fig. 2. Sampling methods for obtaining the RSD values of the species mass concentration. Red particles are API and the rest are excipient.
- Fig. 3. Schematic of the effect of sampling on local segregation and agglomeration of API particles (red colour), Blue particles resemble the excipient.
- Fig. 4. Variation of mass hold-up in the TSM through mixing time, for excipient and API particles.
- Fig. 5. RSD values of the mass concentration of API and excipient particles at $\omega = 500 \text{ rpm}$ and $\Gamma_{AA} = 400 \text{ mJm}^{-2}$. The RSD values are calculated using fine and coarse bins.
- Fig. 6. Comparison between the contact ratios of the API particles with each other at different zones of the mixer.
- Fig. 7. Comparison between the contact ratios of the API and excipient particles at different zones of the mixer.
- Fig. 8. Particles distribution in various sections of the twin screw mixer ($\omega = 500 \text{ rpm}$ and $\Gamma_{AA} = 400 \text{ mJm}^{-2}$).
- Fig. 9. Variation of the API-API and API-excipient contact ratios versus the mixer rotational speed at different mixer zones.
- Fig. 10. A regime map for the blending performance of the twin screw mixer at various surface energies and rotational speeds.

Declaration of interests

The authors declare that they have no known competing financial interests or personal relationships that could have appeared to influence the work reported in this paper.

The authors declare the following financial interests/personal relationships which may be considered as potential competing interests:

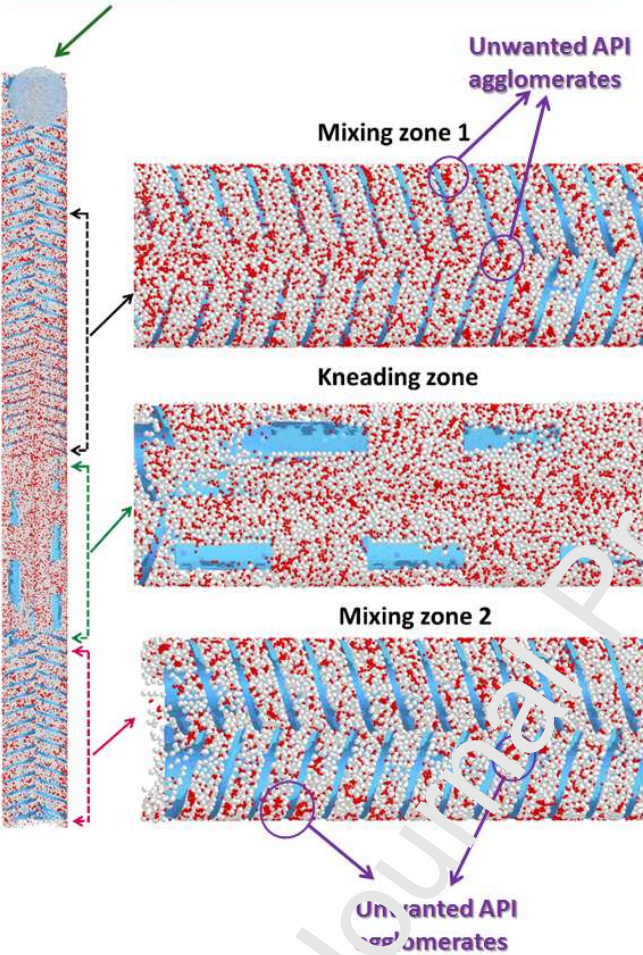
Journal Pre-proof

Coefficient of Blending Performance

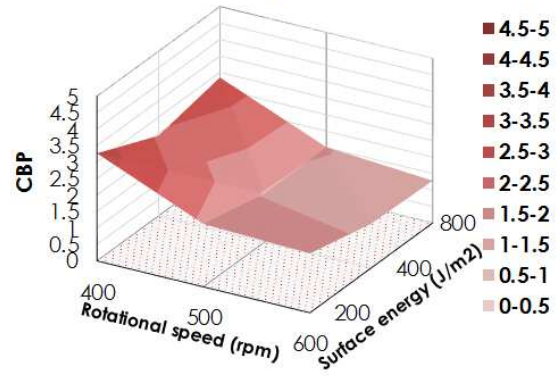
$$= \frac{\text{API} \leftrightarrow \text{excipient contact ratio}}{\text{API} \leftrightarrow \text{API contact ratio}}$$

$$CBP = \frac{N_{A-e}}{N_{A-A}} \cdot \frac{N_A}{N_e}$$

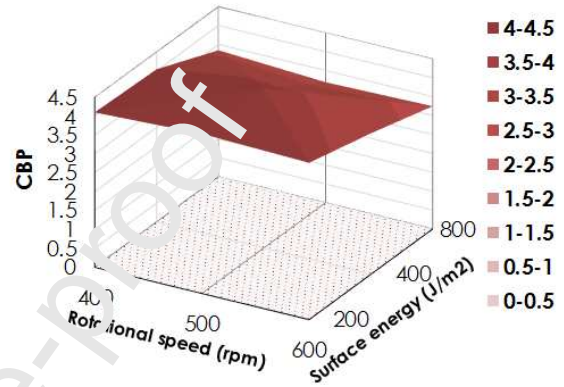
Twin Screw Mixer



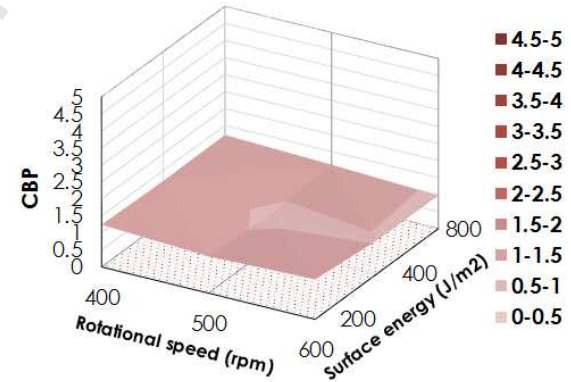
Mixing zone 1



Kneading zone



Mixing zone 2



| Material | API (e.g. Paracetamol) | Excipient (e.g. Lactose) |
|---|------------------------|--------------------------|
| Particle diameter (μm) | 20 | 40 |
| Density (kg/m^3) | ~1200 | ~1500 |
| Young's modulus (GPa) | 9-12 | 11-15 |
| Poisson's ratio | ~0.33 | ~0.30 |
| Surface energy (mJ/m^2) | 40-50 | 40 |

Journal Pre-proof

| Material | API (Paracetamol) | Excipient (Lactose) | Water |
|---|----------------------|------------------------|-------|
| Particle size (μm) | 500 | 1000 | - |
| Density (kg/m^3) | 1200 | 1500 | 7500 |
| Shear modulus (GPa) | 0.1 | 0.1 | 70 |
| Poisson's ratio | 0.30 | 0.30 | 0.25 |
| CoR | 0.01 | 0.01 | 0.01 |
| CoF | 0.5 | 0.5 | 0.5 |
| Generation rate from funnel (g/s) | 0.72 | 7.2 | |
| TSM rotational speed (rpm) | 500, 600, 700 | | |
| Interfacial energy (mJ/m^2) | 200, 400, 800 | | |

| Case | Experiment | DEM1 | DEM2 | DEM3 |
|---|------------|-------|-------|-------|
| Size (μm) | 50 | 500 | 500 | 500 |
| R* (μm) | 25 | 250 | 250 | 250 |
| Interfacial energy (mJ/m^2) | 40 | 200 | 400 | 800 |
| Density (kg/m^3) | 1200 | 2500 | 2500 | 2500 |
| Young's modulus (GPa) | 4 | 0.055 | 0.055 | 0.055 |
| E* (GPa) | 2 | 0.028 | 0.028 | 0.028 |
| Cohesion Number | 2.9 | 0.76 | 2.42 | 7.67 |

Journal Pre-proof

- Continuous blending of pharmaceutical powders in a twin screw mixer is simulated by the Discrete Element Method.
- A kneading and secondary mixing zone is incorporated into the original design.
- A new sample-independent index is proposed to assess unwanted API agglomeration.
- Cohesive Active Pharmaceutical Ingredients (API) form unwanted agglomerates in the mixing zones.
- Adding a kneading zone significantly improves the performance of blending.

Journal Pre-proof